Micellization Study on Block and Gradient Copolymer Aqueous Solutions by DLS and SANS

Satoshi Okabe,[†] Ken-ichi Seno,[‡] Shokyoku Kanaoka,[‡] Sadahito Aoshima,[‡] and Mitsuhiro Shibayama*,[†]

Neutron Science Laboratory, Institute for Solid State Physics, The University of Tokyo, Tokai, Ibaraki 319-1106, Japan, and Department of Macromolecular Science, Graduate School of Science, Osaka University, Toyonaka, Osaka 560-0043, Japan

Received November 1, 2005; Revised Manuscript Received December 15, 2005

ABSTRACT: The dynamic light scattering and small-angle neutron scattering investigations were carried out on aqueous solutions of block (Block) and gradient copolymers (Grad) comprising EOVE and MOVE, where EOVE and MOVE denote 2-ethoxyethyl vinyl ether and 2-methoxyethyl vinyl ether, respectively. Although aqueous solutions of EOVE homopolymer precipitated at 20 °C, the two copolymer systems showed different temperature dependence. A 0.3 wt % Grad system had a micellization temperature range between 20 and 30 °C, while the Block system underwent a sharp transition at around 20 °C. The micellization was continuous in the Grad system, whereas a stepwise transition was observed in the Block system. The resulting micelle size in Grad system was smaller than that in the Block system. The continuous change and the smaller micelle size of Grad were explained by a "reel-in" effect in the micellization process.

Introduction

Block copolymers are known to undergo various types of nanometer-scale structure transitions by self-assembling, such as microphase separation and macrophase separation, depending on the chemical composition, the molecular weight, and the polymer concentration if the polymer is in a solvent.[1,2] These transitions greatly affect the physical properties of the block copolymers, such as viscosity and flow behavior, optical properties, mechanical properties, and gas permeability. To sharpen the changes in the physical properties at the transition point, it is important to choose a combination of unlike constituent blocks as well as to reduce the molecular weight distribution of each block. Recently, Aoshima et al. developed a living cationic polymerization technique providing tailor-made polymers consisting of vinyl ether segments with a desired sequential distribution and architecture. This technique allows one to prepare gradient, graft, and star-shaped copolymers as well as block copolymers with a narrow molecular weight distribution.[3,4] In the previous papers, we discussed the structure and dynamics of block copolymer aqueous solutions in terms of small-angle neutron scattering (SANS) and dynamic light scattering (DLS).[5,6] It was found that an aqueous solution of $pEOVE_{200}$-*block*-$pHOVE_{400}$ undergoes a very sharp thermally induced microphase separation at 20 °C within a narrow temperature range, i.e., a few degrees Celsius, to a microphase-separated structure with a bcc symmetry. Here, pEOVE and pHOVE denote poly(2-ethoxyethyl vinyl ether) and poly(2-hydroxyethyl vinyl ether), respectively. A similar transition was also observed by water addition (a solvent-induced transition) in the case of $pPhOVE_{200}$-*block*-$pMOVE_{400}$ in acetone.[7] Here, pPhOVE and pMOVE denote poly(2-phenoxyethyl vinyl ether) and poly(2-methoxyethyl vinyl ether), respectively.

A gradient copolymer has a concentration gradient along the polymer chain. It is of interest to explore the microscopic behavior of gradient copolymers because an introduction of a concentration gradient to a polymer chain enriches the types of chemical architecture. However, due to the difficulty in controlling the monomer sequence, an "ideal" gradient copolymer had not been obtained. Hashimoto et al. studied tapered block copolymers and classified their characteristic properties by "domain-boundary mixing" and "mixing-in-domain" effects.[8−10] The former represents the case that unlike segments coexist mainly in the domain boundary, resulting in smearing of both the structure and mechanical modulus, and the latter represents the case that the unlike segments coexist even in both domains, leading to a decrease in the concentration difference and a dramatic shift of the transition temperatures. By employing the two concepts, they succeeded in explaining the characteristic features in structural and mechanical properties. Recently, the miscibility criteria and microphase separation in gradient copolymers have been investigated by Lefebvre et al.[11] They predicted that gradient copolymers are less favorable in phase separation and that the size of the microphase separation of gradient copolymers is smaller than that of the corresponding block copolymers. In addition, they also addressed that such microphase separation would hardly occur in bulk. These effects in gradient copolymers may be advantageous in polymer processing. Kim et al. succeeded in compatibilizing polymer blends by adding gradient copolymers during melt processing.[12]

In the present paper, we report essential differences between block and gradient copolymers by investigating the sizes of micelles in aqueous solutions by using DLS and SANS. We employed two copolymers with the same total molecular weights, consisting of the same monomers but different in the chemical sequences, i.e., p(EOVE-*grad*-$MOVE)_{600}$ (Grad) and $pEOVE_{300}$-*block*-$pMOVE_{300}$ (Block) as shown in Figure 1. Here, the numbers indicate the degrees of polymerization. It should be noted that aqueous solutions of pEOVE homopolymer have a clear precipitation point, i.e., LCST (lower critical solution temperature) at around 20 °C.[13] Micellization behavior was carefully compared between aqueous solutions of Grad and Block by analyzing (i) the time−intensity correlation functions

* To whom correspondence should be addressed. E-mail: sibayama@issp.u-tokyo.ac.jp.
[†] The University of Tokyo.
[‡] Osaka University.

10.1021/ma052334k CCC: $33.50
Published on Web 01/26/2006

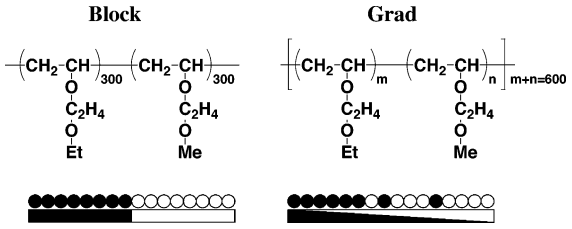

Figure 1. Chemical compositions and schemes for molecular architectures of the copolymers.

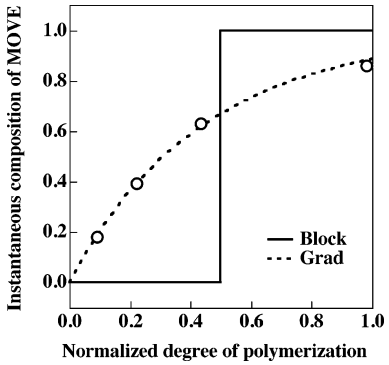

Figure 2. Instantaneous compositions of the Block and Grad along the polymer sequences: broken line, theoretical value; open circle, observed value.

and (ii) the small-angle scattering profiles. An interesting phenomenon, a "reel-in" effect, was observed in aqueous solution of Grad. To our knowledge, this is the first time to observe such an effect in gradient copolymer solutions.

Experimental Section

Samples. Block and gradient copolymers were prepared by living cationic polymerization of MOVE and EOVE with ethyl acetate, as an added base to stabilize the propagating species. The synthesis of diblock copolymers was reported in detail elsewhere.[14] The block copolymer employed in this study has M_n of 5.2×10^4 ($M_w/M_n = 1.25$). The degrees of polymerizations of EOVE and MOVE are both 300. The synthesis of the gradient copolymer was carried out with $CH_3CH(OiBu)OCOCH_3/Et_{1.5}AlCl_{1.5}$ in the presence of ethyl acetate in toluene at 0 °C under dry nitrogen atmosphere.[15] Shortly after living polymerization of the first monomer, EOVE, was initiated, a second monomer, MOVE, was added continuously until the conversion of EOVE reached about 90%. The polymerization proceeded in a living fashion to give a narrow molecular weight distribution with a compositional change along the polymer chain ($M_n = 4.9 \times 10^4$, $M_w/M_n = 1.25$). The composition ratio and the instantaneous composition were determined by ^{1}H NMR spectroscopy (JEOL JNM-EX 270) and gravimetry.[16] Figure 2 shows the observed instantaneous composition of MOVE in a Grad polymer (open circle) and the theoretical one (broken line) as well as that in Block (solid line). The concentration variation of Grad along the polymer chain is markedly different from that of Block. The theoretical curve was calculated from the following equations.[17]

$$-\frac{d[M_1]}{dt} = \frac{r_1 k_{11} k_{22} [M_1][P^*]}{r_1 k_{22}[M_1] + r_2 k_{11}[M_2]} \left\{ [M_1] + \frac{[M_2]}{r_1} \right\} \quad (1)$$

$$-\frac{d[M_2]}{dt} = \frac{r_1 k_{11} k_{22} [M_2][P^*]}{r_1 k_{22}[M_1] + r_2 k_{11}[M_2]} \left\{ \frac{[M_1]}{r_2} + [M_2] \right\} - x \quad (2)$$

where $[M_1]$ and $[M_2]$ are the monomer concentrations (M_1, EOVE; M_2, MOVE), $[P^*]$ is the propagating polymer concentration, k_{11} and k_{22} are the rate constants calculated from first-order plots of homopolymerization of each monomer, r_1 and r_2 are the relative reactivities, and x is the monomer feeding rate. The observed instantaneous composition was in good agreement with the theoretical curve. To clarify the architectures of the resulting micelles, aqueous solutions of Block and Grad with the polymer concentration of 1.0 wt % or 0.3 wt % (coded Block10 and Grad10 or Block03 and Grad03, respectively) were prepared. Deuterated water was used as the solvent in order to enhance the scattering contrast for neutrons.

Light Transmittance. The phase separation temperatures of Grad and Block in aqueous solutions were measured by monitoring the transmittance of a 500 nm light beam through 1.0 cm quartz sample cells at the rate of 1.0 °C/min in heating and cooling scans between 15 and 65 °C. The transmittance was recorded with a JASCO V-500 UV/vis spectrometer with a Peltier-type thermostatic cell holder ETC-505.

DLS. DLS experiments were carried out on a static/dynamic compact goniometer system provided by ALV, Langen, Germany. A 22 mW He−Ne laser with a wavelength of 632.8 nm was used as the incident beam. The scattering angle, θ, was set to be 30, 60, 90, 120, and 138°. The measuring time was 30 s for each sample and condition. The temperature of the sample was regulated with a water-circulating bath (NESLAB RTE-111M). The scattering intensity, $I(\theta, t)$, was monitored as a function of time, t, and was convoluted to obtain intensity correlation functions, $g^{(2)}(\tau)$s, where τ is the correlation time. $g^{(2)}(\tau)$s were then converted to decay rate distribution functions, $G(\Gamma^{-1})$s, by using the CONTIN method, where Γ^{-1} is the characteristic decay time.[18]

SANS. Small-angle neutron scattering (SANS) experiments were carried out at the SANS-U spectrometer owned by the Institute for Solid State Physics, The University of Tokyo, Tokai, Japan.[19] The wavelength of the incident neutrons was monochromatized with a mechanical velocity selector to be 7.0 Å with a distribution of ca. 10% in fwhm. The sample-to-detector distance was chosen to be 2 and 8 m to cover the reciprocal space from 0.005 to 0.2 Å^{-1}. The samples in quartz cells, 1 mm thick, were irradiated by the neutron beam having a cross section 5 mm in diameter. The transmittance of the samples was better than 85% irrespective of temperature for both Block03 and Grad03. The measuring time was varied from 10 to 120 min depending on the samples. The scattered neutrons were collected with a two-dimensional area detector. The scattered intensities were circularly averaged and corrected for transmission and air scattering. The absolute scattering intensity calibration was carried out with the incoherent scattering from a polyethylene secondary standard.[20]

Results and Discussion

1. Light Transmission. Figure 3 shows the temperature dependence for the transmittance at 500 nm light for (a) Block10 and Block03 and (b) Grad10. With increasing temperature, the transmittance of Block10 (Figure 3a) decreased sharply down to below 10% around 20 °C (indicated by the arrow), which is close to the clouding point of pEOVE. This indicates an intermolecular association through aggregation of the pEOVE segments to form micelles. By further increasing the temperature, the polymers precipitated at 60 °C. It is noteworthy that there is little hysteresis between the heating and cooling cycles. This behavior is characteristic of thermosensitive diblock copolymers of vinyl ethers with oxyethylene side groups.[14] The transmittance of Block03, which was used for DLS measurements, indicated that the transmittance was higher than 35% even at the temperature above the LCST. On the other hand, the transmittance for Grad10 (Figure 3b) started to decrease at 23 °C and also exhibited a two-step transition as shown by the arrows. In contrast to Block10, however, the phase separation occurred gradually with a noticeable hysteresis between the heating and cooling cycles. In addition, the transition temperatures (marked with arrows) in the transmittance curve deviated from those for the precipitation points of the two segments, i.e., 20 and 63 °C. Hence, these data clearly indicate that the difference in the architectures between Block and Grad reflects in turbidity behavior.

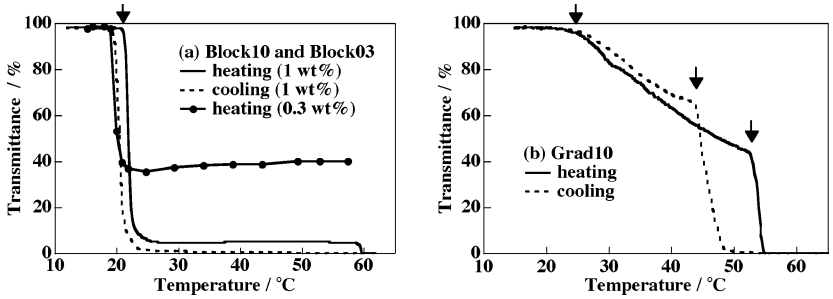

Figure 3. Temperature variations of the light transmittance for (a) Block10 and Block03 and (b) Grad10.

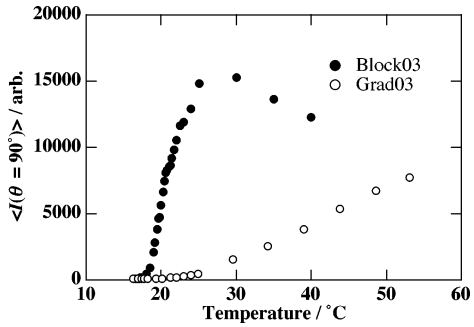

Figure 4. Temperature variations of the light scattering intensity, $I(\theta = 90\ °)$, for Block03 and Grad03.

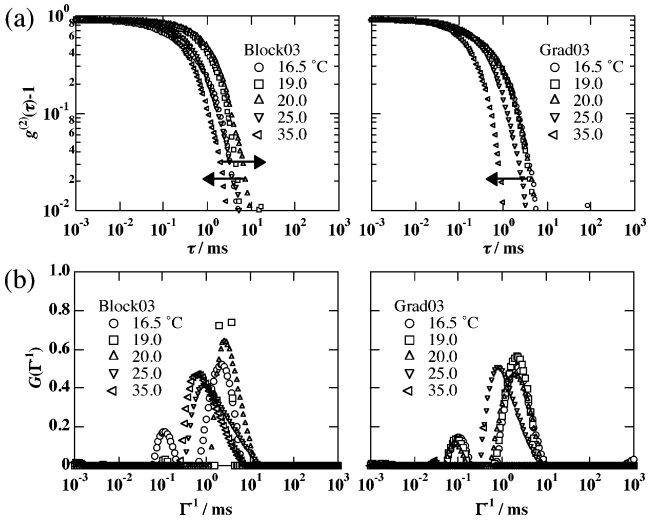

Figure 5. Temperature variations of (a) the intensity correlation functions, $g^{(2)}(\tau)$s, and (b) the distribution functions, $G(\Gamma^{-1})$s, for Block03 and Grad03.

2. DLS. Figure 4 shows temperature dependence of the time-averaged scattering intensities at the scattering angle of 90°, $\langle I(\theta = 90°)\rangle_T$s during the heating process, where $\langle ...\rangle_T$ indicates a time average in 30 s. As reported elsewhere,[6] $\langle I(\theta = 90°)\rangle_T$ for Block03 drastically increased at around 20 °C which was close to the LCST of pEOVE. On the other hand, in the case of Grad03, $\langle I(\theta = 90°)\rangle_T$ increased gradually from rather higher temperature than 20 °C. The difference in temperature dependence of $\langle I(\theta = 90°)\rangle_T$ is well correlated with that of the transmittance.

Figure 5 shows (a) $g^{(2)}(\tau)$s and (b) $G(\Gamma^{-1})$s for Block03 and Grad03. At low temperatures (<20 °C), both systems have two relaxation modes, i.e., the fast and slow modes. However, with increasing temperature, the fast mode of both in Block03 and in Grad03 disappeared as clearly shown by $G(\Gamma^{-1})$s. As for the slow mode, interestingly, there is a clear difference between Block03 and Grad03. With increasing T, the peak of $G(\Gamma^{-1})$ for Block03 shifted to the longer relaxation time and then to the shorter relaxation time. On the other hand, in the case of Grad03, the peak of $G(\Gamma^{-1})$ shifted only to the shorter relaxation time with increasing T. Let us assign the two relaxation modes in the following section.

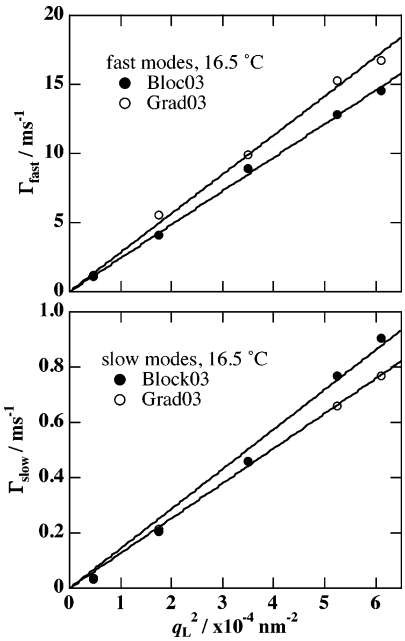

Figure 6. Γ_i vs q_L^2 plots for (a) the fast mode and (b) the slow mode at $T = 16.5$ °C for Block03 and Grad03.

Figure 6 show the Γ_i vs q_L^2 plots for the fast and slow modes at $T = 16.5$ °C, where $q_L = (4\pi/\lambda_L)\sin(\theta/2)$ is the momentum transfer, λ_L is the wavelength of the incident laser light, and θ is the scattering angle. Here, the subscript i denotes either the fast or slow mode (i = fast, slow). The straight lines clearly indicate that the relaxation modes are diffusive. The hydrodynamic radii, $R_{H,i}$s, can be evaluated with the Stokes−Einstein equation

$$R_{H,i} = \frac{kT}{6\pi\eta D_i} \tag{3}$$

with

$$D_i = \frac{\Gamma_i}{q_L^2} \tag{4}$$

where η is the viscosity of the solvent, k is the Boltzmann constant, and T is the absolute temperature, respectively. The diffusion constants, D_is, were obtained as the slopes of the lines in Figure 6. It should be noted here that the linearity of the Γ_i vs q_L^2 plots remained irrespective of temperatures applied in this study. This fact supports the validity of the analysis.

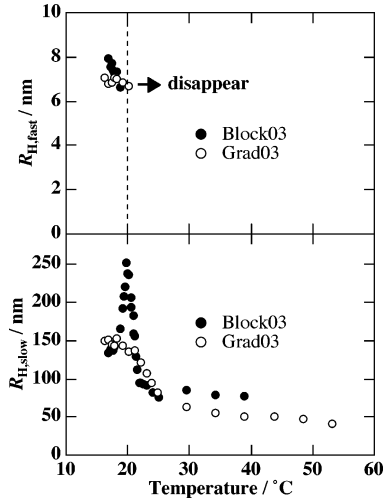

Figure 7. Temperature variations of the hydrodynamic radii, $R_{H,i}$s. The dashed line indicates the temperature at which the fast mode disappeared.

In Figure 7 are shown the variations of $R_{H,i}$s for Block03 and Grad03 during heating process. As shown in the figure, $R_{H,fast}$s for both systems are in the range of 6 to 8 nm at low temperatures (T < 20 °C), corresponding to the translational diffusion of single chains. On the other hand, $R_{H,slow}$ of Block03 and Grad03 was around 150 nm, indicating molecular aggregates. With increasing T, $R_{H,slow}$ of Block03 drastically increased from 150 to 250 nm at around 20 °C and then decreased to be around 80 nm, resulting in micelle formation. This behavior is the same as that of interconnected-chain clusters reported elsewhere (see Figure 10).[6] In the case of Grad03, $R_{H,slow}$ gradually decreased from 150 nm to around 50 nm. The behavior is different between Block03 and Grad03 and the resulting micelle sizes were also different from each other. These facts clearly demonstrate a gradual shrinkage of micelles in Grad03 while a stepwise collapse in Block03. Note that the $R_{H,i}$ values s for Block03 at T > LCST may be distorted by multiple scattering.[21] The validity of the values will be examined in the next section by comparison with the SANS results.

3. SANS. Figure 8 shows the temperature variations of SANS intensity functions, $I(q)$, and fitting results as will be discussed later. Here, q is the momentum transfer defined as

$$q = \frac{4\pi}{\lambda}\sin\left(\frac{\theta}{2}\right), \tag{5}$$

where λ is the wavelength of the incident neutrons. At low temperature (T = 15 °C), $I(q)$s for both systems were monotonically decreasing functions of q. A Guinier analysis was applied to estimate the individual chain sizes. The radius of gyration, R_g can be estimated with,

$$I(q) = I(q=0)\exp\left(-\frac{R_g{}^2 q^2}{3}\right) \tag{6}$$

The evaluated value of R_g was around 7.0 nm both for Block03 and for Grad03. This value agrees with an order estimation for flexible chains with the segment length a = 5 Å and the degree of polymerization Z = 600

$$R_{g,calc} = \frac{aZ^{1/2}}{\sqrt{6}} = 50\ \text{Å} \tag{7}$$

With increasing temperature, the low-q intensity increased and a scattering peak appeared as indicated by arrows. This peak corresponds to micelles formed by dehydration of EOVE-rich segments. The micelle sizes were estimated by using the scattering function for core−shell spheres,

$$I(q) = n|f(q)|^2 \tag{8}$$

$$f(q) = (\rho_{core} - \rho_{shell})V_{core}\Phi(qR_{core}) + (\rho_{shell} - \rho_{solv})V_{core+shell}\Phi(q(R_{core} + L_{shell})) \tag{9}$$

$$V_{core} = \frac{4\pi}{3}R_{core}{}^3 \tag{10}$$

$$V_{core+shell} = \frac{4\pi}{3}(R_{core} + L_{shell})^3 \tag{11}$$

$$\Phi(qR) = \frac{3[\sin(qR) - qR\cos(qR)]}{(qR)^3} \tag{12}$$

where n is the number density of the spheres, ρ_i (i = core, shell, or solv) is the neutron scattering length density of the component i, and R_{core} and L_{shell} are the core radius and shell thickness of the sphere, respectively. Here, the interparticle interference was assumed to be negligible, and accordingly, the structure factor

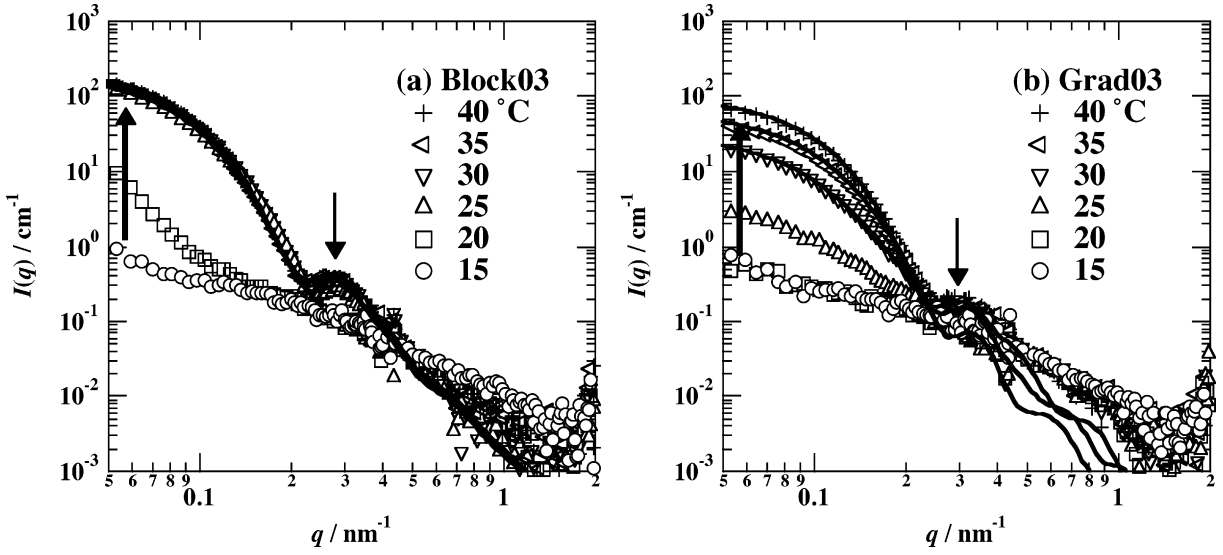

Figure 8. Temperature variations of the SANS intensity functions for (a) Block03 and (b) Grad03. The solid lines are the best fits.

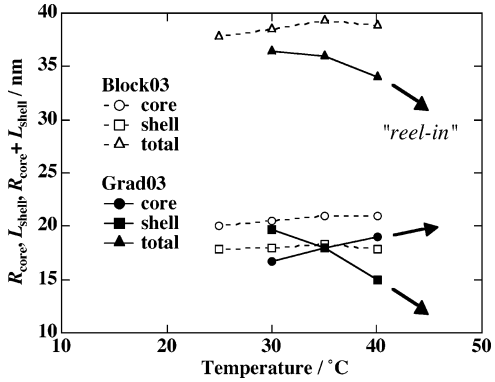

Figure 9. Temperature dependence of the sizes of micelle core and shell.

was not taken into consideration. The solid curves in Figure 8 show the results of curve fitting by considering the instrumental smearing.[5]

The obtained parameters, i.e., R_{core} and L_{shell}, are shown in Figure 9. In the case of Block03 (dashed lines with symbols), there was no significant variation both in R_{core} and in L_{shell} by further heating. This is due to the stepwise change in the sequence of the Block chains, resulting in no morphological change being allowed. In the case of Grad03 (solid lines with symbols), on the other hand, R_{core} increased and L_{shell} decreased gradually with increasing temperature, indicating an increase of the micelle core and a decrease of the corona respectively in Grad03, due to a gradual change in partition of Grad chains to core and corona. The triangles denote the variation of the total lengths, i.e., $R_{core} + L_{shell}$, both for Block03 and Grad03 obtained by SANS, whose temperature dependence are in agreement with $R_{H,slow}$s obtained by DLS.

Now let us estimate the number of copolymer chains participating in a micelle, N, by the following equation.

$$N = \frac{cN_A}{M_w n} \tag{13}$$

where c (g/cm^3) is the mass concentration of the polymer and N_A is the Avogadro's number. The values of n were evaluated by the curve fitting. By using $n = 5.5 \times 10^{13}$ cm^{-3} for Block03 and 5.9×10^{13} cm^{-3} for Grad03, the values of N are obtained to be 630 for Block03 and 620 for Grad03, respectively. These values are in good agreement with that obtained in the similar system.[5]

4. Models for the Micelle Formation in Block and Grad Systems. Figure 10 illustrates models for the structural transitions of Block and Grad in aqueous solutions. At low temperatures (T < 20 °C), the polymer chains are soluble in water and are dispersed in the system by taking an expanded conformation (molecular dispersion, Figure 10, parts 1a and 2a). In the case of the Block system, pEOVE becomes hydrophobic by increasing temperature, resulting in a prompt micelle formation via a transient state of interconnected-chain clusters (Figure 10, parts 1b and 1c). The size of micelles does not change because of the difficulty in further conformational change of EOVE and MOVE segments (Figure 10-1d). On the other hand, EOVE monomers in Grad residing in the gradient fashion start to aggregate at one end of the polymer by increasing temperature, where the fraction of EOVE is relatively higher. As a result, the Grad polymers form micelles with a diffuse interface originated from weaker interaction than that of Block (Figure 10-2b). With increasing temperature, the contribution of the hydrophobic interaction dominates the hydrophobic hydration effect of MOVE segment, just as a reeling in of a fishing wire, resulting in a formation of smaller micelles with larger cores than those of the micelle at lower temperatures (Figure 10-2c). This "reel-in" effect continues to the end of the dehydration of Grad polymers, i.e., LCST of pMOVE, resulting in precipitation of the whole polymers (Figure 10-2d).

Conclusion

Dynamic light scattering (DLS) and small-angle neutron scattering (SANS) investigations were carried out on aqueous solutions of block copolymer (Block) and gradient copolymer (Grad) comprising thermosensitive and hydrophilic monomers. The following facts were disclosed. (1) At low temperature below LCST of pEOVE, both Block and Grad systems have two relaxation modes, i.e., translational diffusions of single chains and molecular aggregates. There are only slight differences in the hydrodynamic radii of these modes between the Block and Grad systems. (2) With increasing temperature, a significant difference between Block and Grad becomes evident. An interconnected-chain cluster was formed in Block system before

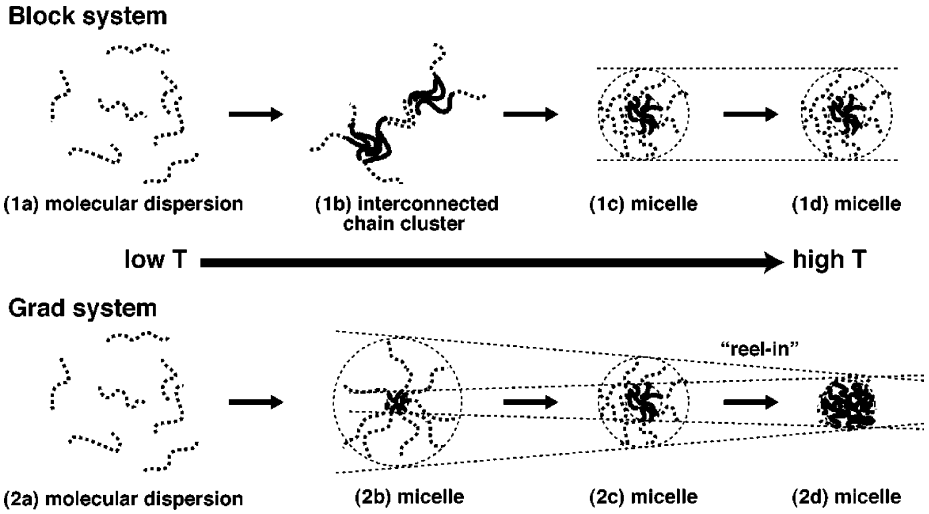

Figure 10. Models for the micelle formation in Block and Grad in aqueous solutions. At low temperature, both Block and Grad polymers are molecularly dispersed in water (parts 1a and 2a). With increasing temperature, a block copolymer micelle (part 1c) is formed stepwise by way of an interconnected-chain cluster (part 1b). The block copolymer micelle hardly changes its size (part 1d). A gradient copolymer micelle (part 2b) gradually shrinks by reeling in its corona and the core increases with increasing temperature (parts 2c and 2d).

reaching compact micelle formation. On the other hand, the aggregate of Grad polymers gradually shrinks to form micelles with large cores. (3) The SANS results clearly show micelle formation with the core sizes of 39 nm for Block system and around 36 nm for Grad system, which has significant temperature dependence. Furthermore, the total size of the micelle decreases with temperature exclusively in Grad system. It can be concluded that the variation of micelle size in Grad system is ascribed to the "reel-in" effect. Gradient copolymer micelles can attract (or reel in) their coronas much more strongly than block copolymer micelles. This is due to the gradient nature of the monomer composition along the Grad chain.

Acknowledgment. This work was partially supported by the Ministry of Education, Science, Sports, and Culture, Japan (Grant-in-Aid No. 14350493 and 14045216 to M.S.). SANS experiments were carried out under the approval of the neutron scattering program, the Institute for Solid State Physics, the University of Tokyo (Proposal No. 05.259).

References and Notes

(1) Zhang, L.; Eisenberg, A. *Science* **1995**, *268*, 1728.
(2) Hamley, I. W. *The Physics of Block Copolymers*; Oxford University Press: Oxford, U.K., 1998.
(3) Aoshima, S.; Higashimura, T. *Macromolecules* **1989**, *22*, 1009−1013.
(4) Aoshima, S.; Sugihara, S.; Shibayama, M.; Kanaoka, S. *Macromol. Symp.* **2004**, *215*, 151−163.
(5) Okabe, S.; Sugihara, S.; Aoshima, S.; Shibayama, M. *Macromolecules* **2002**, *35*, 8139−8146.
(6) Okabe, S.; Sugihara, S.; Aoshima, S.; Shibayama, M. *Macromolecules* **2003**, *36*, 4099−4106.
(7) Fuse, C.; Okabe, S.; Sugihara, S.; Aoshima, S.; Shibayama, M. *Macromolecules* **2004**, *37*, 7791−7798.
(8) Tsukahara, Y.; Nakamura, N.; Hashimoto, T.; Kawai, H.; Nagaya, T.; Sugimura, Y.; Tsuge, S. *Polym. J.* **1980**, *12*, 455−466.
(9) Hashimoto, H.; Tsukahara, Y.; Kawai, H. *Polym. J.* **1983**, *15*, 699−711.
(10) Hashimoto, H.; Tsukahara, Y.; Tachi, K.; Kawai, H. *Macromolecules* **1983**, *16*, 648−657.
(11) Lefebvre, M. D.; Cruz, M. O.; Shull, K. R. *Macromolecules* **2004**, *37*, 1118−1123.
(12) Kim, J.; Gray, M. K.; Zhou, H.; Nguyen, S. T.; Torkelson, J. M. *Macromolecules* **2005**, *38*, 1037−1040.
(13) Aoshima, S.; Oda, H.; Kobayashi, E. *J. Polym. Sci., Part A: Polym. Chem.* **1992**, *30*, 2407−2413.
(14) Aoshima, S.; Sugihara, S. *J. Polym. Sci., Part A: Polym. Chem.* **2000**, *38*, 3962−3965.
(15) Tsujimoto, I.; Aoshima, S. *Polym. Prepr. Jpn.* **2002**, *51*, 194.
(16) Yoshida, T.; Kanaoka, S.; Watanabe, H.; Aoshima, S. *J. Polym. Sci., Part A: Polym. Chem.* **2005**, *43*, 2712−2722.
(17) Mayo, R. F.; Lewis, M. F. *J. Am. Chem. Soc.* **1944**, *66*, 1594−1601.
(18) Peters, R. In *Dynamic Light Scattering: The Methods and some Applications*; Brown, W., Ed.; Oxford University Press: Oxford, U.K., 1993.
(19) Okabe, S.; Nagao, M.; Karino, T.; Watanabe, S.; Shibayama, M. *J. Appl. Crystallogr.* **2005**, *38*, 1035−1037.
(20) Shibayama, M.; Nagao, M.; Okabe, S.; Karino, T. *J. Phys. Soc. Jpn.* **2005**, *74*, 2728−2736.
(21) Pine, D. J.; Weitz, D. A.; Maret, G.; Wolf, P. E.; Herbolzheimer, E.; Chaikin, P. M. In *Scattering and localization of classical waves in random media*; Sheng, P., Ed.; World Scientific: Singapore and Teaneck, NJ, 1990; pp 312−372.

MA052334K